

Diamond: Nesting the Data Center Network with Wireless Rings in 3D Space

Yong Cui¹, Shihan Xiao¹, Xin Wang², Zhenjie Yang¹, Chao Zhu¹, Xiangyang Li^{1,3}, Liu Yang⁴, and Ning Ge¹

¹Tsinghua University

²Stony Brook University

³University of Science and Technology of China

⁴Beijing University of Posts and Telecommunications

Abstract

The introduction of wireless transmissions into the data center has been shown to be promising in improving the performance of data center networks (DCN) cost effectively. For high transmission flexibility and performance, a fundamental challenge is to increase the wireless availability and enable fully hybrid and seamless transmissions over both wired and wireless DCN components. Rather than limiting the number of wireless radios by the size of top-of-rack (ToR) switches, we propose a novel DCN architecture, *Diamond*, which nests the wired DCN with radios equipped on all servers. To harvest the gain allowed by the rich reconfigurable wireless resources, we propose the low-cost deployment of scalable 3D Ring Reflection Spaces (RRSs) which are interconnected with streamlined wired herringbone to enable large number of concurrent wireless transmissions through high-performance multi-reflection of radio signals over metal. To increase the number of concurrent wireless transmissions within each RRS, we propose a precise reflection method to reduce the wireless interference. We build a 60GHz-based testbed to demonstrate the function and transmission ability of our proposed architecture. We further perform extensive simulations to show the significant performance gain of Diamond, in supporting up to five times higher server-to-server capacity, enabling network-wide load balancing, and ensuring high fault tolerance.

1 Introduction

The high-performance data center network (DCN) is an essential infrastructure for cloud computing. There is a quick growth of large-scale services (e.g., Google Search, Hadoop, MapReduce, etc.) in the cloud, and recent measurements show tremendous traffic variations over space and time in DCNs [5, 7, 8, 20]. Conventional wired DCNs generally adopt the fixed and symmetric network design. This may lead to prevalent hot spots

across different layers of the architecture which significantly reduces the performance of DCNs [7, 20, 37].

There are some recent interests on constructing *hybrid* DCNs [18, 19, 33, 38, 39] with the introduction of new network components such as optical circuit switches or wireless radios into the DCNs to provide configurable links [9, 13, 25, 28]. Although these hybrid infrastructures show the potential in achieving higher DCN capacity and lower transmission delay, their wired structures are kept unchanged even though they are not primitively designed to work with new network techniques, which limits the performance of hybrid DCN. Specifically, the new network components are added directly into conventional DCNs or are applied to replace part of existing network switches [18, 33, 38, 39]. Considering only the *local* performance improvement, it is hard for existing schemes to achieve the global optimal performance in the presence of network-wide traffic changes. The key challenge of a *fully hybrid* network design is to form a novel hybrid network architecture that can take full advantage of different network techniques and enable coherent and seamless transmissions for much higher DCN performance.

The low cost of today's commodity 60GHz radios makes their wide deployment a better option in a fully hybrid network design [39]. Providing high wireless availability in the data center is the key to achieving high performance gain in a hybrid architecture. In existing proposals for hybrid DCNs, wireless radios are generally deployed on a flat 2D plane at the top of racks, which is susceptible to signal blocking [38]. Although a flat reflector on the room ceiling was proposed to alleviate the problem [19, 38], the ceiling height is quite restricted (3 meters [38]) and the method requires clearance above racks, which is usually infeasible in conventional data centers. The small rack size also restricts the number of radios that can be placed on each rack (at most eight radios per rack [38, 39]). If radios are densely deployed on top of racks, the strong inter-radio interference would restrict the number of concurrent wireless links thus con-

straining the system performance [39]. The need of deploying more radios and links in the hybrid network for higher wireless availability calls for a completely new DCN architecture design.

In this work, we propose a novel *fully-hybrid* network architecture, named Diamond, which ensures high wireless availability for efficient and high-performance DCN communications. Rather than restricting the radios to be on top of racks, we propose to deploy wireless radios along with a large number of servers. To avoid the interference among dense radios at the 2D plane, we propose to construct multiple **Ring Reflection Spaces** (RRSs) to make the radios sparsely distributed in the 3D space. Inside each RRS, we develop a novel multi-reflection method to address the blocking problem on building wireless links. With our design, there is no need of changing the room plan above racks. Diamond has three key design features:

Novel hybrid network topology (§2): Rather than adding wireless radios directly on top of racks, we propose a fully hybrid network topology by constructing RRSs in Diamond to facilitate wireless transmissions and isolate the wireless interference. It also supports direct server-to-server wireless links rather than conventional rack-to-rack links. Then we apply a streamlined wired herringbone to interconnect the RRSs at low cost.

Precise multi-reflection of wireless links (§3): The susceptibility to blocking and the interference are two major issues that limit the wireless performance in DCNs. To the best of our knowledge, this is the first work that develops the multi-reflection transmission method to address the challenge of signal blocking. We further design a novel precise reflection scheme to efficiently restrict the wireless interference in the presence of a large number of concurrent wireless links.

Wireless & wired hybrid routing (§4): We propose an opportunistic hybrid routing scheme to allow for low transmissions delay and graceful fault tolerance. We further show that the network diameter of Diamond can scale logarithmically with the server number to effectively bound the route length.

We implement a 60GHz-based testbed, and our experimental results confirm the high performance of multi-reflection, and demonstrate that proper reflection holes can efficiently reduce the interference in 3D space (§6). Driven by the testbed parameters, our simulations show that Diamond can support up to five times higher server-to-server capacity and ensure graceful fault tolerance (§7). Finally, we introduce the related work (§8) and draw the conclusions (§9).

2 Architecture

In this section, we first introduce the basic architecture and methodologies used in the Diamond system, and

then present its hybrid topology design.

2.1 Diamond system overview

At a high level, the Diamond system should meet the data center needs at different timescales. First, the configuration of wireless links should be updated periodically so that the network topology can better accommodate the current traffic of the data center. Second, given a configured network, we need to efficiently route the flows in real time.

Dynamic wireless configuration: Following the prior studies, the Diamond system exploits the controller of software-defined networking (SDN) for flexible and efficient configuration of the wireless links and routing paths [4, 11, 26, 27]. More specifically, the Diamond controller periodically updates the configuration of the wireless links based on the traffic conditions reported from SDN-controllable ToR switches. Servers are equipped with high-capacity wireless radios (60GHz radio [18] or FSO transceivers [19]). To dynamically configure the wireless links, they are allowed to communicate with each other either directly by steering and aligning the antennas (physically or electronically driven [18, 19]) or using a multi-reflection method we propose. The controller first builds wireless links to alleviate the heavy traffic from the hot spots, and then randomly forms additional wireless links using the remaining available radios to achieve the benefits of random networking [31].

Hybrid routing: The controller only computes the routing paths of hot-spot server pairs during the wireless configuration to alleviate the hot-spot traffic globally for the network-wide load balancing thus higher network throughput. For other light-loaded server pairs, the routing decision is made distributedly by servers and switches so that their traffic can go through available wireless links opportunistically to cut short the routing paths in real time.

2.2 Key methodologies

There are two main challenges to implement a fully hybrid network: (1) When a large number of wireless links are enabled, the interference will restrict the number of concurrent transmissions; and (2) When a large number of wireless radios are deployed, the high-frequency wireless links are easily blocked by obstacles such as the supply pipes of air conditioning or the steel structures above racks. In light of these problems, Diamond applies a 3D deployment of the wireless radios to facilitate high number of concurrent wireless transmissions taking advantage of the following key techniques:

Space division multiplexing: To disperse the wireless radios, the radios in Diamond are installed with servers at different heights. Rather than deploying the wireless

radios densely on only one flat 2D plane, we place the wireless radios on several separated large annular surfaces. Thus the deployment density of wireless radios is much lower than that of previous studies [38, 39]. The adjacent annular surfaces form a RRS where the signal can run from one radio to another. Due to the space division, the same set of wireless channels can be multiplexed across different RRSs, which helps isolate the interference in Diamond.

Multi-reflection transmission: Although more radios can be deployed in a 3D space, many radios cannot reach each other with existing direct point-to-point transmission or the one-reflection transmission [18, 19, 38, 39] due to the obstacle blocking. Instead, in Diamond, we utilize multiple reflections to bounce the signal emitted from one server to another. This helps to greatly increase the number of available wireless links. Following the prior work [38], our testbed experiment confirms that using the flat metal board as reflector can offer very good specular reflection with little energy loss or changing path loss during each reflection. This avoids the overhead of buffering and switching packets in multiple hops over intermediate switches.

Different types of directional antennas may have different beam widths [18]. For a multi-reflection path, there is a tradeoff between the antenna beam width and the tolerance for the antenna alignment error. The narrower the beam width, the higher the antenna gains, but the less the alignment error tolerance. In the extreme case of using FSO with nearly zero beam width, previous study shows that using electrically-driven Galvo mirrors is possible to implement precise steering control [19]. For conventional 60GHz antennas, the electrically-driven antenna array is promising to satisfy this requirement [18, 39].

Precise reflection technology: Since the wireless antenna may have a wide beam width [18], multiple reflections would introduce unexpected interference inside the 3D space due to the signal leakage of the beam (e.g., the undesired side lobes of the 60GHz wireless beam [18, 29]). In order to efficiently restrict and control the interference caused by reflections, we develop a precise reflection method with the careful placement of absorbing materials on the reflection boards. Most areas of the board are covered by absorbing paper while small holes are left so that only the intended signal reflections are made by hitting the hole, which leads to very little signal leakage.

2.3 Topology design

The basic *motivation* of the Diamond topology design is to enable more concurrent wireless transmissions. In our design, we separate the specific transmission functions of wireless and wired links in the network, so that both

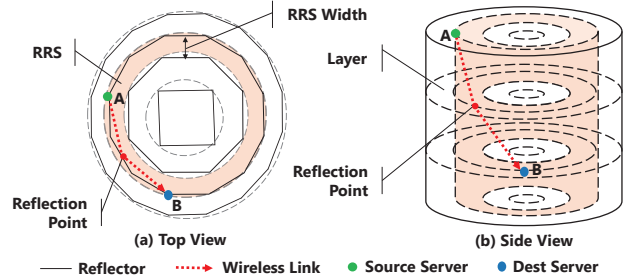


Figure 1: Brief view of the wireless ring in Diamond ($N=4$ rings and $H=4$ layers)

their distinct advantages on the transmission can be fully explored. We construct a ring-shape basic structure that enables wireless-only transmissions inside the ring employing the multi-reflections (§2.2). Then we apply the stable wired links to address the transmissions across different ring structures.

From the top view in Fig. 1, Diamond’s topology is constructed by several concentric regular polygons with increasing radius. Polygons are numbered from inside to outside and named by *rings*, i.e., $\{R_i\}$, $1 \leq i \leq N$, where N is the total number of polygons. The i_{th} ring has $4i$ edges. The racks are placed at the vertex points of each ring, and there are totally $\sum_{1 \leq i \leq N} (4i) = 2(N^2 + N)$ racks, while flat metal reflectors are put at the edge of each ring. Rather than mounting the reflectors [19, 38] on the ceiling, reflectors in Diamond stand in perpendicular to the ground and have the same height as that of racks, which avoids the need of using clear ceiling space for wireless transmissions in data centers. In the following, we introduce the designs of major Diamond components.

Server and rack. Each rack holds multiple servers at different height. The servers inside different racks at the same height form a *layer*, and the layers are numbered from the top to the bottom as $\{l_j\}$, $1 \leq j \leq H$. The height of each layer equals the height of a server at conventional racks, and the number of layers H equals to the number of servers in one rack. Therefore, a Diamond topology can accommodate totally $2(N^2 + N)H$ servers. Each server is equipped with 1 Ethernet port and 2 wireless ports with directional antennas. The networking principles in Diamond are: (1) the links between two servers are wireless; (2) the links between a server and its ToR switch or between two ToR switches are wired.

Wireless links: The 3D space between two neighboring rings is called an RRS. For each server, one of its antennas points to RRS at its inner side and the other points to RRS at its outer side. By adjusting the antenna directions in the RRS, each server at ring R_i can flexibly communicate with other servers at different heights on rings R_i , R_{i-1} and R_{i+1} through direct transmissions or multiple reflections on different reflectors (Fig. 1 and Fig. 3).

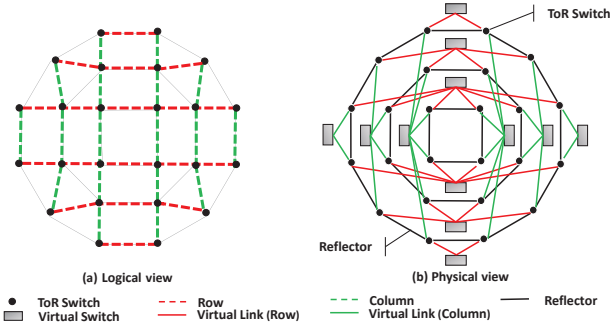


Figure 2: Top view of the wired herringbone of Diamond ($N=3$ rings)

Wired links: With wireless links formed locally inside each RRS, the wired links are applied to interconnect different RRSs. Fig. 2 gives a top view of the wired connections in Diamond. Similar to conventional DCNs, the servers on each rack are connected to the common ToR switch. Fig. 2(a) shows the logical view of the *wired herringbone*. We number the horizontal lines in Fig. 2(a) from the top to the bottom as rows $\{r_i\}$, $1 \leq i \leq 2N$, and number the vertical lines from the left to the right as columns $\{c_i\}$, $1 \leq i \leq 2N$. Fig. 2(b) shows the physical connections of the wired herringbone. The principle of Diamond to interconnect the RRSs is that the ToR switches on the same row (or column) are interconnected by a *virtual switch*, while the ToR switches on different rows and different columns are not directly connected.

To implement the function of virtual switch, we have the option of applying any existing structure, e.g., the tree-based structure (Fat-tree [3]) or cube-based structure (BCube [16]), to interconnect the ToR switches on each row and each column. These structures may make the wired design of Diamond complex and costly. In Diamond, we prefer to apply the de-Bruijn graph [12] so that no additional switches are required. De-bruijn is attractive for providing constant link degree at each node and logarithmic network diameter. Then the path length is bounded and the routing structure is still simple (§4). Although using de-Bruijn structure often involves complex wiring [17], the wiring is kept simple in Diamond because only one row (or column) of ToR switches are connected as one de-Bruijn.

2.4 Rack and reflector arrangement

There are two requirements to arrange the racks in Diamond to facilitate its practical and scalable deployment: first, all the reflector boards should be flat and have the same length to facilitate their economical production; second, the RRS width should be kept stable, with the RRS width close to a fixed value when the number of rings increases. We call the physical distance between two neighboring rings R_i and R_{i+1} as the RRS width Δ_i (Fig. 1). Too large a RRS width will make Diamond oc-

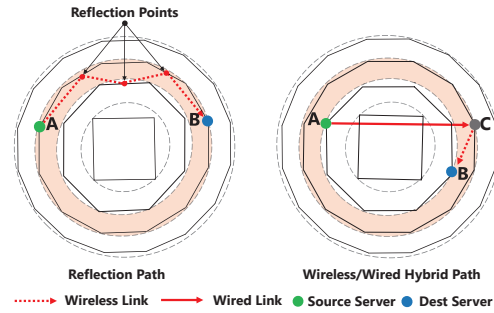


Figure 3: Routing in the 3D wireless ring

copy too much room area, while too small a RRS width will not leave enough space for wireless transmissions.

As mentioned earlier, all the polygons in Diamond are regular with the same edge length and are put concentrically in a symmetric way as shown in Fig. 2. The reflector height equals the height of racks, and the reflector length is denoted as L . Then our design ensures the RRS width Δ_i at i th ring to have the following property:

Property 1. $\lim_{i \rightarrow \infty} \Delta_i = 2L/\pi$

Proof. Based on the topology of Diamond, the radius d_i of ring R_i is $d_i = (\cot \frac{\pi}{4i}) \frac{L}{2}$. Then we have $\Delta_i = d_{i+1} - d_i = (\cot \frac{\pi}{4(i+1)} - \cot \frac{\pi}{4i}) \frac{L}{2} = \frac{\sin(\frac{\pi}{4} \frac{1}{i(i+1)})}{\sin[(\frac{\pi}{4})^2 \frac{1}{i(i+1)}]} \frac{L}{2}$. Hence we have $\lim_{i \rightarrow \infty} \Delta_i = 2L/\pi$.

Based on the above proof, the RRS width Δ_i decreases as the ring number i becomes larger. Property 1 ensures that the RRS width does not fall to zero but reaches a fixed limit value. For a setting $L=2.5\text{m}$, the RRS width Δ_i can keep a value close to the fixed limit value 1.6m. We can see that the RRS width becomes stable and approaches the fixed limit value quickly when the ring number increases, which demonstrates the scalability of the Diamond design.

3 Wireless configuration

In this section, we first introduce our schemes of finding the reflection path when building a wireless link and eliminating the wireless interference during the reflections, and then present our strategies in forming flexible wireless configurations for network-wide load balancing.

3.1 Reflection path

Since the physical topology of Diamond is fixed, the reflection paths can be easily calculated between any two servers. The calculation of the reflection path table is done offline at the initial deployment of Diamond. If there are multiple paths available between two servers, we choose the one with the least number of reflection

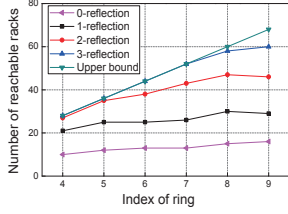


Figure 4: Number of reachable racks per server at different rings and within different reflection times

times (direct transmission is considered as zero times of reflection). Given a source server and a destination server in Diamond, if a reflection path can be found in the table, the antenna angles can be adjusted by the servers according to the table values to build the wireless link.

Based on the Diamond topology, we simulate the reflection paths between all the server pairs. Fig. 4 shows the average communication range of a wireless radio, i.e., the reachable rack number at both its current ring R_i and inner ring R_{i-1} . We can see that no more than three reflections can cover above 90% racks in the RRS when the ring number is less than 9. For a ring number larger than 4, a server can reach at least 10 racks through the direct transmission, 20 racks within a single reflection and 28 racks within two reflections.

3.2 Reduction of wireless interference

We design a precise reflection method to alleviate the wireless interference during reflections. Specifically, we carefully place the absorbing materials on the reflection board and leave small *holes* for only the intended reflection points. In the following, we analyze the density and distribution of reflection points (i.e., the reflection holes) on the reflector boards.

To simplify the analysis, we first present a special *circle case* where the flat reflectors are replaced by curved reflectors so that all the polygons are transformed to their circumcircles. We consider the communication of servers inside the k th RRS, i.e., the communication between a server on ring k and another on ring $k+1$ and the communication between two servers on ring $k+1$. The reflection times are limited within three. The communication of servers in different rings is achieved by zero and double reflections. The double reflection forms the reflection points on the outer side of ring k and the inner side of ring $k+1$.

Considering the distribution of reflection points on ring k , we have the following property:

Property 2. *At each layer of Diamond, for an arbitrary reflector on ring k , there are at most six reflection points on the reflector board.*

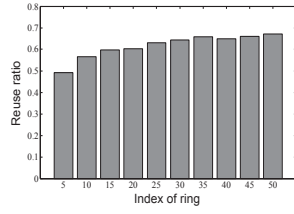


Figure 5: Reuse ratio of reflection points on a board at different rings

Proof. *Based on the coordinates of a server n on ring $k+1$ and a server m on ring k , we obtain the central angle for each reflection point, denoted as $\frac{2}{3} \cdot \frac{\pi(2n-1)}{4(k+1)} + \frac{1}{3} \cdot \frac{\pi(2m-1)}{4k}$, $m, n \in \mathbb{Z}^+$. We shift the value of m and n to find the minimum change of the central angle of the reflection point. The minimum change $\frac{\pi}{12k}$ is the minimum interval of two reflection points. As the central angle for the reflector on ring k is $\frac{\pi}{2k}$, there are at most six reflection points at each layer of the reflector board. This completes the proof.*

We obtain the expressions of the central angle for each reflection point in ring $k+1$ following the same procedure of ring k . We examine the distribution of reflection points on each reflector in ring $k+1$ based on simulation results, and found that at each layer from the ring 5 to the ring 50, there are average ten reflection points on the board of the ring $k+1$. One hole may be reused by a large number of reflection points for different reflection paths, i.e., the distance between two reflection points is small enough to overlap with each other. With the reuse ratio equal to the ratio of reused points to the total number of reflection points, Fig. 5 shows that the reuse ratio is high and increases when the ring number becomes larger.

3.3 Configuration for hot-spot traffic

Since the above techniques enable a large number of server-to-server wireless links, Diamond can implement a network-wide reconfigurable topology for balancing the identified hot-spot traffic, which contributes to high throughput and effective routing.

Configuration problem: The wireless configuration is determined by the network controller in DCNs. The controller input is a traffic demand matrix where an entry describes the traffic demand between a pair of servers. Given a hybrid topology G , we can construct its *interference graph* G_I^1 to describe the conflict relations among all the wireless links based on offline measurements [18]. The objective of our wireless configuration is to select the optimal *independent set* (IS)² to minimize the maximum link utilization of the entire network during each scheduling period. We thus have an integer linear programming (ILP) problem HLBP (Hybrid Load Balance Problem). Our HLBP problem mainly differs from previous study Firefly [19] on the additional wireless interference constraint on IS selections. Finding all the ISs is NP-complete in general [14]. We find that even the state-of-art ILP solver LINGO or ILP toolbox in MATLAB may take above tens of minutes to solve the HLBP.

¹The *independent graph* G_I of G is defined as a graph where each link in G corresponds to a vertex in G_I , and if two links have conflict in G , then there is a link between them in G_I .

²An *independent set* (IS) in an interference graph G_I is defined as a vertex subset where any two vertices do not conflict.

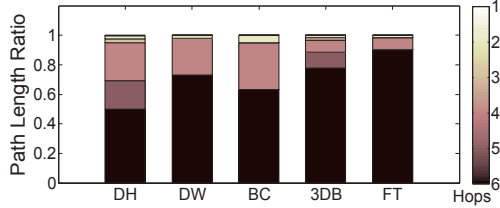


Figure 6: Path length ratio of different topologies

There are some existing studies [21–23, 34–36] on finding an approximate IS solution in some special interference graphs. In the following, in order to make Diamond support various types of antennas, we turn to the development of a fast heuristic solution for a general interference graph.

Greedy scheduling: We design a greedy algorithm HDF (Highest Demand First) to provide a faster and simpler solution for HLBP. The algorithm assigns a weight value to wireless links related to the flows, and then selects a set of non-conflict wireless links that maximize the sum of weights. We define the weight of a wireless link as the ratio between the flow demand and the link length. For a link with reflections, the link length is the total geometric length of the reflection path. The intuition is that a link can provide larger benefit when serving higher flow demand over a shorter link length, as a shorter wireless link allows for smaller interference range and higher SNR thus higher link capacity. We greedily select the links with the largest weight to build first and remove the links that conflict with the selected links. Next, the traffic demands are split into their shortest paths. Denote the minimum remaining capacity of links along a path as the *path capacity*. The server pair with the highest demand first splits the traffic to transmit over the set of shortest paths in proportional to the path capacity. Then the remaining link capacities are updated and the procedure repeats until no server pair is left. The gap between HDF and the optimal solution is evaluated in §7.

3.4 Random networking for high capacity and low delay

Since the wireless resources are rich in Diamond, after offloading the hot-spot traffic by HDF, some wireless radios may be left unused, particularly when the number of hot spots in the network is not big in a scheduling period. Random networking is shown to have the features of small average path length, high path diversity and high server-to-server network capacity [31, 32]. Thus we expect that the random formulation of wireless links helps to shorten the path length in Diamond.

To verify this effect, we compare the percentage of the path length for all the server pairs under different DCN topologies with 512 servers in Fig. 6. DH is for Diamond where wireless links are built randomly; DW is for Diamond with the wired connections only; BC is the BCube

topology [16]; FT is the Fat-tree topology [3]; 3DB is a Fat-tree topology augmented by 3D-beamforming radios at ToR switches [38]. We can see that the number of long paths in DW is larger than that in BCube. However, when introducing random wireless links, the ratio of short paths in DH is higher than all the other topologies. The short path length generally implies small hop delay and high end-to-end throughput due to fewer congestion points at intermediate routing hops [31, 32].

To benefit from the random networking in Diamond, we extend the IS selected by the HDF algorithm to a *maximal* IS, named the MIS, by randomly adding additional wireless links into the IS without creating conflict until no such kind of wireless link is available. The random formulation of wireless links in Diamond avoids the problem of complex wiring and costly management appearing in the previous work on using random wired links in DCNs [32].

4 Routing Design

Diamond is built upon a topology-adaptive network, while existing routing protocols often impose a relatively long convergence time when the topology changes [6]. For more efficient routing, we propose to use a set of strategies in Diamond.

4.1 Overall scheme

The setup of wireless links is performed by the Diamond controller periodically. We denote the time interval for the controller to execute the wireless reconfiguration as one *period*. At the beginning of each period, a set of operations will be performed as follows: (1) The controller computes the wireless configuration and the routing paths for hot-spot server pairs using the methods described in §3, and sends out the instructions to both servers and their associated ToR switches. (2) The servers receiving the configuration instructions will adjust their antenna directions accordingly.

To summarize, there are three choices for a server or ToR switch to route its traffic. First, a server or ToR switch tries to match the routing rules designated by the controller. If matched, it delivers the packet accordingly. This first choice helps to balance the hot-spot traffic following the controller’s decisions. Otherwise, it opportunistically utilizes its available wireless radios (if it is a server) or the available radios on its rack (if it is a ToR switch) to create a short-cut hop to the destination. This second choice contributes to shorter routing path through opportunistic hybrid routing. If no wireless radios are proper to use, it delivers the packet to the next-hop node following a default wired routing path. This last choice efficiently bounds the worst-case performance by routing through the wired herringbone.

4.2 Default wired routing

For the Diamond topology introduced in §2.3, a 3-tuple (x, y, z) labels a server at the x th row, y th column and z th layer. For simplicity, we use a 3-tuple $(x, y, 0)$ to label a ToR switch on the x th row and y th column. Fig. 7 shows a simple example to route from an arbitrary source server $s_1 = (x_1, y_1, z_1)$ to a destination server $s_2 = (x_2, y_2, z_2)$. Let $w_1 = (x_1, y_1, 0)$ and $w_2 = (x_2, y_2, 0)$ denote their corresponding ToR switches respectively. The shortest wired routing path can be established as follows. First, the packet routes from s_1 to w_1 and then we change one of the two coordinates of source ToR switch w_1 at a time to match that of switch w_2 : $(x_1, y_1, 0) \rightarrow (x_2, y_1, 0) \rightarrow (x_2, y_2, 0)$. Finally, the packet routes from w_2 to s_2 . Note that each coordinate change corresponds to hops through a virtual switch.

Suppose we apply de-Bruijn structure to implement the virtual switch, and the Diamond topology has totally $H = 2p$ layers and N rings. Then we need $4p$ ports per ToR switch, where $2p$ ports connect to the servers on the rack and $2p$ ports are used for constructing the de-Bruijn on its row and column. Since the diameter of a de-Bruijn graph is $\log_p N$, the path length through a virtual switch (i.e., the path length between two ToR switches on one row or column) can be bounded by $\log_p N$. Based on the above routing procedure, we have the property:

Property 3. *The network diameter, which is the longest shortest path among all the server pairs, of Diamond is bounded by $2\log_p N + 2$.*

Since the Diamond with H layers and N rings can support totally $n = 2(N^2 + N)H$ servers, we have the diameter of Diamond as $O(\log_p n)$. Compared to conventional approaches (e.g., the Fat-tree [3] or VL2 [15] topology) which has a constant diameter but the number of switch ports increase with the number of servers, Diamond has much better scalability. As the server number increases, its network diameter extends logarithmically while the port number can be kept as a constant. This is similar to the recursion-based DCN topology such as BCube [16] and DCell [17]), which also has a logarithmic diameter when keeping a constant number of switch ports.

4.3 Opportunistic hybrid routing

The wired herringbone of Diamond provides the basic assurance of the connectivity and route length bound. Now we integrate the wireless transmissions into the default wired paths opportunisticly. Suppose a server $s_1 = (x_1, y_1, z_1)$ receives a packet for a server $s_2 = (x_2, y_2, z_2)$, and the ToR switches of s_1 and s_2 are $w_1 = (x_1, y_1, 0)$ and $w_2 = (x_2, y_2, 0)$. The server s_1 is equipped with two radios, which are pointed to servers $s'_1 = (x_3, y_3, z_3)$ and $s''_1 = (x_4, y_4, z_4)$, respectively. Define

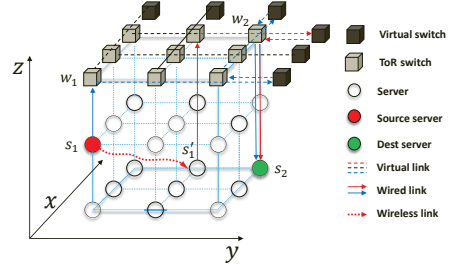


Figure 7: Opportunistic hybrid routing in Diamond

a **hamming distance** $\mathcal{D}(s_1, s_2)$ as the number of the unmatched coordinates between the tuples s_1 and s_2 . Then the value range of $\mathcal{D}(s_1, s_2)$ is $\{0, 1, 2, 3\}$.

To perform the *opportunistic hybrid routing* (OHR), each server in Diamond simply follows two steps for the packet forwarding: (1) Call $d_1 = \mathcal{D}(s_1, s_2)$. If all three are matched (i.e., $d_1 = 0$), then it is the destination server. (2) Call $d'_1 = \mathcal{D}(s'_1, s_2)$ and $d''_1 = \mathcal{D}(s''_1, s_2)$. If $d'_1 < d_1$ or $d''_1 < d_1$, forward the packet to the server s'_1 or s''_1 accordingly through a wireless radio. Otherwise, forward the packet to the switch w_1 by default.

Similar to the servers, each ToR switch in Diamond forwards the packet as follows: (1) Call $d_1 = \mathcal{D}(w_1, s_2)$. If the first two are matched (i.e., $d_1 = 1$), it forwards the packet to s_2 directly; Otherwise, it randomly chooses one coordinate among the unmatched ones. Assume that ToR switch picks x_1 where $x_1 \neq x_2$, then the default next hop is $w_f = (x_2, y_1, 0)$. (2) For each server s_i in the rack, suppose its wireless radios point to two servers s'_i and s''_i . Call $d'_i = \mathcal{D}(s'_i, s_2)$ and $d''_i = \mathcal{D}(s''_i, s_2)$. If $d'_i < d_1$ or $d''_i < d_1$, forward the packet to the sever s_i in the rack; Otherwise, forward the packet to the ToR switch w_f by default.

4.4 Fault-tolerance

The redundancy of available paths between any pair of servers make Diamond attractive for fault-tolerance. There are two types of failures to handle in Diamond: node failure and link failure. Three classes of node failure should be considered: (a) switch failure, (b) server failure and (c) wireless radio failure. A link failure will be resulted from a node failure, or the change of the environment such as the blocking of wireless communications due to the human movement in the RRSs. Clearly, due to the nested structure of Diamond, any single node or link failure does not lead to the network disconnection. We describe link failures here because other node failures trigger the same responses.

In Diamond, each server has three different output links to forward the packets: (a) forward to the ToR switch it connects to; (b) forward to one of its two wireless radios. When a server finds one of its output links fails, it removes that wired/wireless connection from its

connection list, and chooses one of the remaining available output links as its next hop based on the routing rules described in Section 4.3. Benefited from the distributed routing property of OHR, the routing paths can be recovered quickly in Diamond to ensure high fault tolerance.

5 Discussion on deployment issues

Circle vs. Polygon reflector. We have so far suggested using the flat mental board as the reflector to facilitate its economic production and easy deployment. If the cost is not a concern, however, a curved mental reflector would allow the wireless communication range of each server to be larger than that of the flat reflector for the same constraint on reflection times. Considering that the curved reflectors are used to construct the circumference of each ring, with the ring number varying from 5 to 100 and the reflection times set to be within three, we find that the average wireless communication range per server in the polygon case is above 80% that of the circle case. When the number of rings is smaller than 5, both cases ensure the communications of all the servers of the entire ring. The results indicate that using flat reflector is a better choice for the deployment in a large-size data center.

Design of virtual switch. Diamond introduces a virtual switch to interconnect the ToR switches on a line (row or column) and the virtual switch can be implemented by any existing interconnection structures, e.g., the tree-based structure [3, 15] or cube-based structure [2, 16], with different trade-offs between the cost and performance. However, the number of ports required by a virtual switch on different rows and columns may not be the same in Diamond. Consider a Diamond topology with $2n$ rows and $2n$ columns, the port numbers of virtual switch from row r_1 to r_n are $\{2, 4, 6, \dots, n-2, n\}$. The uneven port numbers make it difficult to deploy conventional interconnection structures as some structures do not scale continuously [3, 16, 17]. To address this issue, we suggest using one virtual switch to interconnect two rows (or two columns) together to make a balance of the port number. Then each virtual switch requires $n+2$ ports by combining every two rows as (r_1, r_n) , (r_2, r_{n-1}) , (r_3, r_{n-2}) and so on. We can obtain the same result as that of $2n+1$ rows and columns by excluding the median row and column.

Rack density and wireless link number. To provide an idea of the deployment density of Diamond, we give an example. A room of data center with the size $100 \times 100 m^2$ can hold 2k racks if using Diamond, and

hold 3.7k racks if using the conventional row-based architecture, so the density of the conventional architecture is about 1.8 times that of Diamond. The lower rack density in Diamond ensures a proper space for both the wireless transmissions and cooling when the network scales up. However, our simulation results with different room sizes of a data center show that, the server-to-server throughput in Diamond on average doubles that of a conventional three-layer fat-tree DCN topology for the same room size [3]. As Fig. 4 shows, if we limit the reflection times of a path to be less than two, for a medium-size data center with 1000 servers, there will be more than 0.1 million potential wireless links available for use. The rich wireless links contribute a lot to the network-wide adaptive topology formulation and can support efficient routing and fault-tolerance in Diamond.

Cabling complexity. The cabling complexity is an important issue to consider in the deployment of DCNs. Despite their contributions to big performance improvements, both the tree-like topologies [3] and recursion-based topologies [16, 17] introduce complex cabling among racks and thus high maintenance cost in practice. This is because the physical row-by-row rack deployment does not work well with their logical tree or recursive topologies. In contrast, the cabling in Diamond is much easier with its wired structure simplified to be several rows and columns both logically and physically. As Fig. 2(a) shows, the row lines and column lines are independent from each other and thus are simple for both cabling and maintenance.

Cooling and maintenance. Heat dissipation is important for a data center to run healthily. In conventional DCN architectures, the most challenging heat issue comes from the closely placed racks in multiple rows. Since the rack density in Diamond is both lower and more balanced (i.e., the distance between any two neighboring racks is similar) than conventional architectures, the heat is distributed more evenly and lightly. For better cooling effect in Diamond, we suggest piping the cooling air from bottom to top in each ring. In addition, we suggest leaving four gaps at the polygon corners evenly on each ring to form four tunnels through the innermost to the outermost, through which the engineers can go inside each ring for device maintenance. When there is human moving inside, some wireless links may be blocked and failed. However, Diamond can handle the failure of wireless links easily (§4.4) and fast redirect the flows to wired links until the wireless link is available again.

Moreover, the antenna steering delay may be an issue to affect the system performance. The delay of steering 60GHz antenna can potentially be controlled within 250us if using phase array technology [18], while if deploying FSO in Diamond, the steering delay can be within 0.5ms using Galvo mirrors [19]. To further alleviate

Table 1: Total cost of different DCN architectures

Topology #	Cost (k\$)					Power (kw)
	NIC	Switch	Radio	Wire	Total	
FatTree	80	2080	-	80	2240	3486
3DB	80	2080	192	80	2432	3486
FireFly	80	416	2400	16	2912	4281
Diamond	240	832	1920	32	3024	3428

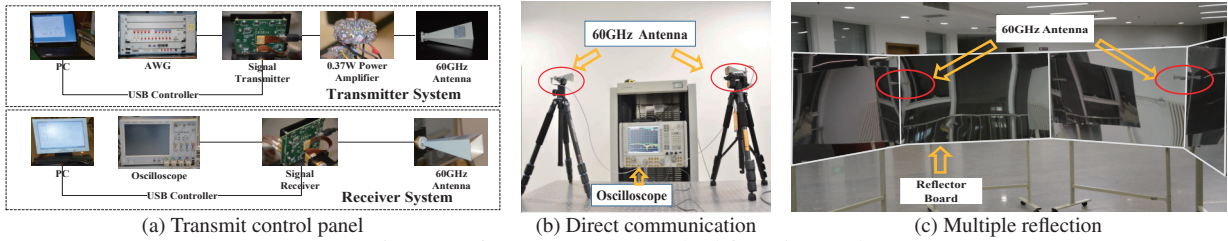


Figure 8: 60GHz antenna testbed for Diamond

the side effect, our system ensures that the transmissions through wireless links during the antenna steering to be easily migrated to the stable wired links.

Deployment cost. A set of hybrid DCNs are proposed recently, such as the 3D-beamforming(3DB) [38] (8 radios per rack) and FireFly [19]. We use Fat-tree to represent the conventional wired architecture and compare the cost of different architectures in Table. 1. We consider the cost and power of NICs on the server, switches, wireless radios and wires. We conservatively estimate each wireless radio costs \$60 [39], each 40-port switch costs \$1040, each port in the NIC costs \$5 and needs 5W [16], each port in the FSO device costs \$150 [19], and an average cost of \$1 per meter for cabling [19] and \$1 per square meter of absorbing paper. We assume the reflectors used in Firefly, 3DB and Diamond have negligible cost. All the architectures hold 16 thousand servers. We can see that although Diamond uses a large number of radios, its cost is only 24% higher than that of 3DB because it uses 60% fewer switches. This trade-off is reasonable as a larger number of wireless links are enabled in Diamond than 3DB. Firefly can offer higher bandwidth at a higher deployment cost. However, the ceiling mirror it requires may not be applicable in most modern data centers. An alternative solution is to replace 60GHz radios in Diamond with FSO devices, which will provide similar performance as Firefly without the need of deploying ceiling mirrors but at a higher deployment cost.

6 Implementation

We implement a 60GHz testbed to evaluate the transmission performance of our architecture under different wireless communication conditions.

Experiment setup: To demonstrate the feasibility of 60GHz wireless communication in our architecture, we build a testbed (Fig. 8a) to carry out the relevant experiments. The testbed was composed by Vubiq Networks Inc’s commercial millimeter wave transceiver components, self-designed 60GHz Power Amplifier and AINFO Inc’s 60GHz rectangular waveguide horn antenna. The system enables 60 GHz experiments on the use of integrated transmitter/receiver waveguide modules. 60GHz Power Amplifier is placed at the end of the transmitter to increase the transmission power. It has

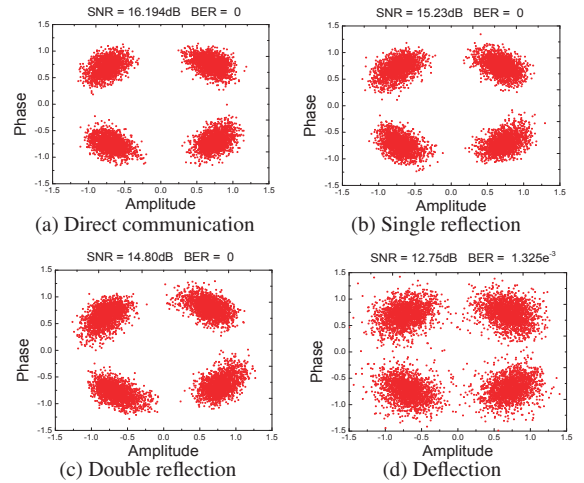


Figure 9: Measured constellation diagram: performance of different transmission ways

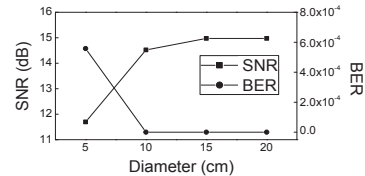


Figure 10: Performance over different hole sizes

a gain of 30dB and a saturated output power of 0.37W. The testbed encodes the data file with LPDC and applies the QPSK modulation to generate the waveform. The receiver module samples the signal and recovers the original data file.

We first carry out four experiments, including the direct communication, communication through single reflection, communication through double reflections and communication through deflection (i.e., the misalignment of two communicating antennas). In this group of experiments, to ensure the transmission ability of the architecture, the distance between the sender radio and the receiver radio is set to 25 m. The communication rate is 2.5 Gbps and the LPDC encoding rate is 3/4. We show the results in Fig. 9. For the second group of experiments, we change the hole size to test the performance of precise reflection for both the single and double reflection cases. To make an accurate measurement of hole size, the distance between the sender and receiver is set to 3m. The results are presented in Fig. 10 and Fig. 11.

Experiment result on signal reflection: As Fig. 9

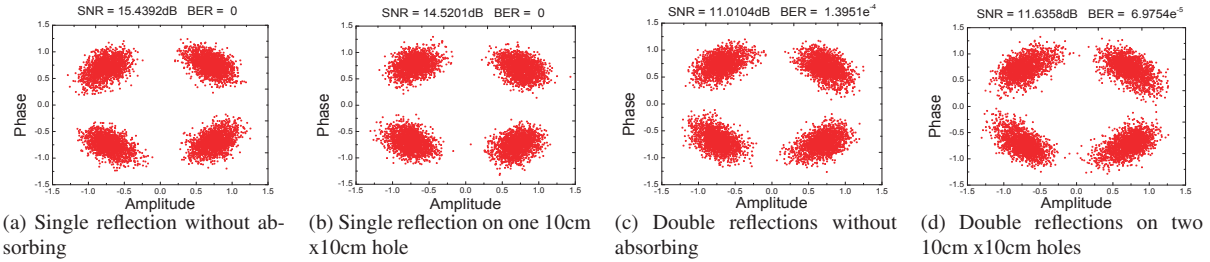


Figure 11: Measured constellation diagram: performance of precise reflection

shows, the direct communication and the communications through single reflection and double reflections present a good communication quality and the corresponding SNR are 16.194 dB, 15.23 dB and 14.80 dB respectively. For all the experiments on our testbed, the measured data rates of both the directional and reflectional 60GHz links are shown to keep a value above 2.5Gbps over a distance of 25m. Therefore, the bandwidth of 60GHz wireless link is high enough for multiple-gigabit data transmissions in Diamond.

Experiment result on receiver alignment: During the measurement, we find that the communication quality through deflection changes with the deflection angle between two radios. As Fig. 9d shows, when the deviation angle becomes 20° , the SNR is 12.75 dB, which is the critical value of the communication quality. When the deviation angle further increases, the communication quality becomes too bad for the receiver to decode the original data. This indicates that our 60GHz radio is highly directional and has a small main-lobe width less than 20° , which contributes to a small angular interference to other radios when constructing the wireless interference graph. At the same time, the main-lobe angle provides a certain degree of fault tolerance on the antenna alignment between two servers in Diamond. We studied the impact of antenna misalignment through simulation with the above experimental parameters as input, and our result show that the average flow throughput drop is within 10% when the misaligned degree is within $\pm 20^\circ$, which demonstrates that Diamond has a good tolerance to the fault as a result of the misalignment of antennas.

Experiment result on the precise reflection: We examine the impact of hole size on the reflector and show the single-reflection performance in Fig.10. We are not showing the results with hole size larger than 20cm, because they are the same as the 20cm case. We can see that when the hole size is 10cm, the SNR gets a slight decrease but BER is kept at zero. When the hole size further decreases to 5cm, the SNR drops quickly and results in the transmission failure.

After obtaining the proper hole size as 10cm, we measure the constellation diagram for both the single and double reflections. Fig. 11(a) and Fig. 11(c) show the results of reflections without any absorbing materials on

the reflector. Fig. 11(b) and Fig. 11(d) show the corresponding results with one 10cm x10cm hole on each reflector. We can see that the transmission performance keeps nearly the same for both cases. Another interesting finding is that for double reflections, the SNR even gets slightly better when the reflectors are full of absorbing paper with only one hole left. The gain may be achieved as a result of the reduction of the multiple-path interference with the use of absorbing material. This demonstrates the feasibility of using precise reflection in Diamond.

7 Simulation

Setup and workloads. Our simulations are performed by a customized flow-level simulator. We use the same settings of TCP for the flow-level simulator as that utilized in [4], where the additive increase factor of flow rate is set to 15 MB/s. The wireless transmission follows the general physical interference and path loss model [10]. The related wireless parameters, such as the signal fading due to the misalignment of antennas, are all set following the testbed-based measurement results shown in Section 6.

For comparative analysis, we consider two classes of typical DCN topologies respectively: (1) wired topology and (2) hybrid topology. In the first part, we evaluate the performance of the wired backbone of Diamond (named Diamond-Wired) and other typical wired DCN topologies. The wired link capacity is set to 1Gbps, and we use Fat-tree [3] and BCube [16] as the representatives for the tree-based DCN topology and the recursion-based DCN topology respectively. In the second part, we evaluate the performance of Diamond and the state-of-art hybrid architecture 3D-beamforming [38]. We apply Fat-tree as the oversubscribed core for 3D-beamforming. Since 3D-beamforming deploys the wireless radios only at the ToR layer, to make a fair comparison, we apply two radios on top of each rack for both 3D-beamforming and Diamond. Thus, only the first layer of servers in Diamond are equipped with wireless radios and the radio numbers are the same for both topologies. To compare the performance only under distributed routing, we further disable the HDF (Highest Demand First algorithm) function and only use the OHR (Opportunistic Hybrid

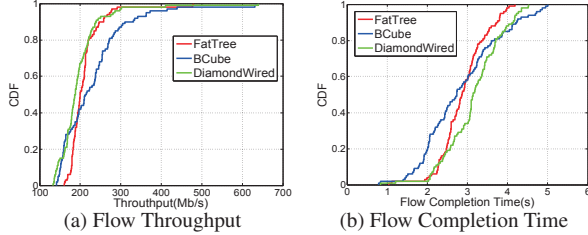


Figure 12: Flow Performance of Wired Architectures

Routing) routing in Diamond (named Diamond-OHR), while 3D-beamforming uses ECMP routing. Limited by the memory space of our simulator, the number of rings in Diamond is set to six.

To compare the performance on load balancing and fault tolerance, we evaluate Diamond and other DCN topologies under different traffic patterns and number of node failures. The HDF routing and wireless radios are all enabled for Diamond (named Diamond-HDF) in the comparison cases. We transfer 200 random flows with their sizes set within 200MB, and show the performance results of flow throughput and flow completion time.

Performance of wired architecture. In Fig. 12a, we can see that BCube performs the best while Diamond-Wired has similar flow throughput as Fat-tree. The number of flows whose throughput is larger than 300Mbps takes 10% in BCube, while the percentage is less than 1% in the other two topologies. This is because that DiamondWired simplifies its wired backbone by using much fewer switches and wires. Similar trends on the performance of flow completion time can be found in Fig. 12b.

Performance of hybrid architecture. Consider the original traffic as long flows. We add another 200 random short flows (whose average size is one tenth that of the original traffic) to study the performance of mixed flows in hybrid architectures. In Fig. 13a, the throughput of long flows in Diamond-OHR is higher than that of 3D-beamforming. The number of long flows whose throughput is larger than 225Mbps takes above 90% in Diamond, while the number takes less than 40% in 3D-beamforming. Moreover, in Fig. 13b, the maximum completion time of short flows in Diamond is about 25% less than that of 3D-beamforming. In Diamond, a larger number of concurrent wireless links can be supported to increase the transmission capacity, which contributes to both higher throughput for long flows and smaller completion time for short flows.

Performance of load balancing. Following the prior work [19], we use a uniform model where flows between pairs of racks arrive independently with a Poisson arrival-rate as the baseline. We also consider the hotspot model [23], where in addition to the uniform baseline, a subset of rack pairs have higher arrival rates and larger flow sizes. We use a tuple (X, Y) to describe the hotspot traffic model: the X element represents the average flow

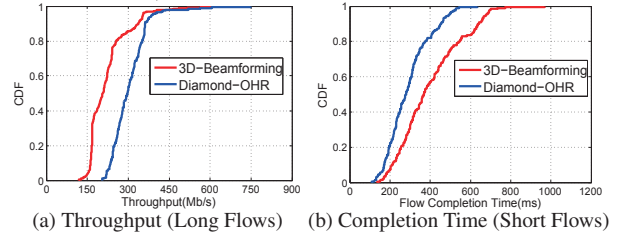


Figure 13: Flow Performance of Hybrid Architectures

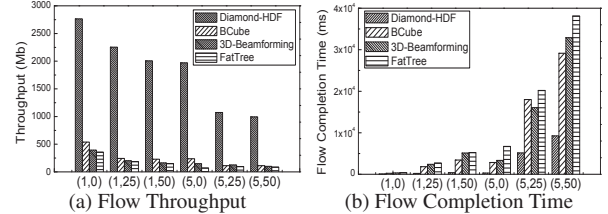


Figure 14: Flow Performance for Traffic Patterns

size, where 1 denotes the average flow size is 100MB, and 5 corresponds to 500MB; the Y element denotes the percentage of the number of hot nodes.

As Fig. 14 shows, the flow performance of the four topologies deteriorates as expected when increasing the average flow size and the number of hot nodes. Diamond-HDF performs the best, providing the largest flow throughput and lowest flow completion time. Benefited from the rich server-level wireless links, the throughput of Diamond is about 5 times that of other topologies in the lightest traffic case (1,0), and 9 times that of the other topologies in the worst traffic case (5,50). Correspondingly, the flow completion time of Diamond is about 70% lower than that of other topologies. This demonstrates the high performance gains of Diamond-HDF and its capability of effectively balancing the load upon heavy traffic.

Performance of fault tolerance. In Fig. 15, we evaluate the flow performance of Diamond-HDF and Diamond-Wired when different percentages of nodes fail. To ensure that every flow can be routed under the node failures, we first randomly disable certain percentage of nodes and then randomly generate 100 flows to transmit for the remaining nodes. As Fig. 15 shows, the flow throughput of both the Diamond-HDF and Diamond-Wired decreases with the increasing node failure ratio. However, the flow throughput of Diamond-HDF decreases much slower than that of Diamond-Wired. Considering the failure ratio from 0% to 20%, the flow throughput of Diamond-HDF decreases about 13% while Diamond-Wired decreases about 28%. This illustrates the graceful performance degradation of Diamond-HDF for node failures. Similar trends on flow completion time can be found in Fig. 15b.

Performance of wireless reconfiguration. In Table 2, we compare the computation delay and performance of the greedy solution HDF in Diamond with the optimal

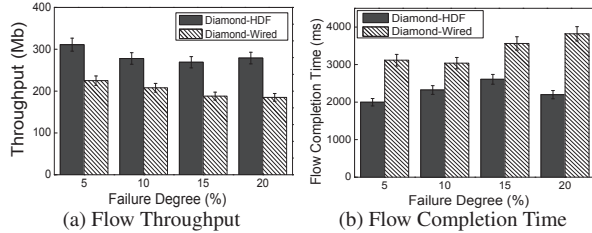


Figure 15: Flow Performance for Fault Tolerance

solution (named Full-ILP) of the HLBP problem. We use the ILP solver LINGO to compute the global optimal solution of ILP for routing (we obtained the same results when using the ILP toolbox in MATLAB for calculation). Limited by the memory constraint of LINGO, we evaluate the scales of Diamond with up to 5 rings which contains totally 60 racks and each rack holds 48 servers. We can see that the computation delay of Full-ILP increases quickly with the number of rings while HDF keeps a stable and low computation delay around 30ms. The tradeoff is HDF gets up to 15% gap on the performance of throughput and flow completion time when compared with Full-ILP. For a practical network scale within 20 rings, Full-ILP can not provide the solution in reasonable time, while HDF still achieves a low delay within 100ms, which is comparable to the feasible scheduling overhead illustrated in [4].

8 Related Work

Conventional data center: There exist prevalent hot spots in hierarchical data centers [3, 15, 18, 39], which limits the DCN performance. Many DCN architectures have been proposed to address the hot-spot problem in tree-based data center networks. Some efforts [30–32] propose to construct a random networking topology to achieve smaller network diameter, less hot spots and higher performance than state-of-art structured architectures. But the wiring and routing are quite challenging in a totally random wired network. In [16, 17], authors propose to build the network recursively to efficiently eliminate the structured bottleneck. However, the routing is restricted to follow its recursive structure, which does not consider the high dynamics in traffic demands and thus may lead to more hot spots.

Hybrid data center networking: Recent efforts turn to hybrid data center networking with flexible new networking components (e.g., the optical circuit switches, 60GHz wireless radios or FSO transceivers) to address the dynamic traffic demands [13, 18, 19, 24, 25, 28, 33, 38].

Table 2: Performance of reconfiguration

Ring #	Delay (ms)		Throughput Gap	Flow Completion Time Gap
	Full-ILP	HDF		
2	219	15	0.08	0.11
3	313	31	0.08	0.15
4	625	31	0.12	0.01
5	11625	32	0.15	0.15

Flyway first illustrates the feasibility of applying 60GHz wireless technology in DCNs [18]. The work in [38] further enhances the Flyway performance by using the ceiling reflector to bounce signals to avoid blocking on the 2D plane. Using the same method, Firefly explores the feasibility of running free-space-optical (FSO) transmissions in DCNs [19]. This method, however, requires a height-restricted ceiling and also complete clearance above racks, which is infeasible in most data centers due to the existence of air conditioning pipes and steel structures above the racks [1]. Moreover, existing methods only considered the local performance improvement at the rack level and part of network layers. In contrast, Diamond can run a larger number of network-wide wireless links (either 60GHz or FSO) without involving any engineering efforts to change the room plan above racks. Both wireless technologies can be applied in Diamond at the server level with different trade-offs: commodity 60GHz antenna is much cheaper and smaller than FSO transceivers while FSO has little interference footprint and longer transmission distance. With the decreasing cost of optical transceivers, FSO shows great promise to run in Diamond in the future.

9 Conclusion

We propose Diamond, a novel hybrid network architecture, to enable high capacity and seamless data transmissions over both wired and wireless network links. Specifically, we introduce the concept of Ring Reflection Space (RRS) to enable the wide deployment of wireless radios at servers and high number of concurrent wireless transmissions through low-cost multi-reflection over the metal, and develop a precise reflection scheme to reduce the wireless interference inside an RRS. The rich wireless resources allow Diamond to flexibly configure the network topology and form the transmission path to avoid creating hot traffic spots while enabling transmissions over random network topology for low delay. We also prove the scalability of the proposed architecture. We implement the proposed techniques over 60GHz testbed and demonstrate its functionality. Our results from extensive simulations show that the cohesive structure of Diamond enables fine-grained and network-wide load balancing, effective routing and graceful fault-tolerance.

Acknowledgments

This work is supported by National Natural Science Foundation of China (no. 61120106008, 61422206), Tsinghua National Laboratory for Information Science and Technology (TNList). Xin Wang’s research is supported by NSF CNS 1526843, and Xiangyang Li’s research is supported by NSF ECCS-1247944. We would like to thank our shepherd Alex C. Snoeren and the anonymous reviewers for their valuable feedback and suggestions.

References

- [1] Google data center image. <http://www.google.com/about/datacenters/gallery/#/all>.
- [2] ABU-LIBDEH, H., COSTA, P., ROWSTRON, A., O'SHEA, G., AND DONNELLY, A. Symbiotic routing in future data centers. In *SIGCOMM* (2011).
- [3] AL-FARES, M., LOUKISSAS, A., AND VAHDAT, A. A scalable, commodity data center network architecture. In *SIGCOMM* (2008).
- [4] AL-FARES, M., RADHAKRISHNAN, S., RAGHAVAN, B., HUANG, N., AND VAHDAT, A. Hedata: Dynamic flow scheduling for data center networks. In *NSDI* (2010).
- [5] ALIZADEH, M., GREENBERG, A., MALTZ, D. A., PADHYE, J., PATEL, P., PRABHAKAR, B., SENGUPTA, S., AND SRIDHARAN, M. Data center tcp (dctcp). In *SIGCOMM* (2011).
- [6] BASU, A., AND RIECKE, J. Stability issues in ospf routing. In *SIGCOMM* (2001).
- [7] BENSON, T., AKELLA, A., AND MALTZ, D. A. Network traffic characteristics of data centers in the wild. In *IMC* (2010).
- [8] BENSON, T., ANAND, A., AKELLA, A., AND ZHANG, M. Understanding data center traffic characteristics. *ACM SIGCOMM Computer Communication Review* 40, 1 (2010), 92–99.
- [9] CHEN, K., SINGLA, A., SINGH, A., RAMACHANDRAN, K., XU, L., ZHANG, Y., WEN, X., AND CHEN, Y. Osa: an optical switching architecture for data center networks with unprecedented flexibility. In *NSDI* (2012).
- [10] CUI, Y., WANG, H., CHENG, X., LI, D., AND YLÄ-JÄÄSKI, A. Dynamic scheduling for wireless data center networks. *IEEE Transactions on Parallel and Distributed Systems (TPDS)* 24, 12 (2013), 2365–2374.
- [11] CURTIS, A. R., MOGUL, J. C., TOURRILHES, J., YALAGANDULA, P., SHARMA, P., AND BANERJEE, S. Devoflow: scaling flow management for high-performance networks. In *SIGCOMM* (2011).
- [12] DE BRUIJN, N. G., AND ERDOS, P. A combinatorial problem. *Koninklijke Nederlandse Akademie v. Wetenschappen* 49, 49 (1946), 758–764.
- [13] FARRINGTON, N., PORTER, G., RADHAKRISHNAN, S., BAZZAZ, H. H., SUBRAMANYA, V., FAINMAN, Y., PAPAN, G., AND VAHDAT, A. Helios: a hybrid electrical/optical switch architecture for modular data centers. In *SIGCOMM* (2011).
- [14] GAREY, M. R., AND JOHNSON, D. S. Computers and intractability: A guide to the theory of np-completeness. *WH Freeman & Co., San Francisco* (1979), 61–62.
- [15] GREENBERG, A., HAMILTON, J. R., JAIN, N., KANDULA, S., KIM, C., LAHIRI, P., MALTZ, D. A., PATEL, P., AND SENGUPTA, S. V12: a scalable and flexible data center network. In *SIGCOMM* (2009).
- [16] GUO, C., LU, G., LI, D., WU, H., ZHANG, X., SHI, Y., TIAN, C., ZHANG, Y., AND LU, S. Bcube: a high performance, server-centric network architecture for modular data centers. In *SIGCOMM* (2009).
- [17] GUO, C., WU, H., TAN, K., SHI, L., ZHANG, Y., AND LU, S. Dcell: a scalable and fault-tolerant network structure for data centers. In *SIGCOMM* (2008).
- [18] HALPERIN, D., KANDULA, S., PADHYE, J., BAHL, P., AND WETHERALL, D. Augmenting data center networks with multi-gigabit wireless links. In *SIGCOMM* (2011).
- [19] HAMEDAZIMI, N., QAZI, Z., GUPTA, H., SEKAR, V., DAS, S. R., LONGTIN, J. P., SHAH, H., AND TANWER, A. Firefly: a reconfigurable wireless data center fabric using free-space optics. In *SIGCOMM* (2014).
- [20] KANDULA, S., SENGUPTA, S., GREENBERG, A., PATEL, P., AND CHAIKEN, R. The nature of data center traffic: measurements & analysis. In *SIGCOMM* (2009).
- [21] LI, X.-Y. Multicast capacity of wireless ad hoc networks. *IEEE/ACM Transactions on Networking (TON)* 17, 3 (2009), 950–961.
- [22] LI, X.-Y., TANG, S.-J., AND FRIEDER, O. Multicast capacity for large scale wireless ad hoc networks. In *MOBICOM* (2007).
- [23] LI, X.-Y., AND WANG, Y. Simple approximation algorithms and ptass for various problems in wireless ad hoc networks. *Journal of Parallel and Distributed Computing* 66, 4 (2006), 515–530.
- [24] LIU, H., LU, F., FORENCICH, A., KAPOOR, R., TEWARI, M., VOELKER, G. M., PAPAN, G., SNOEREN, A. C., AND PORTER, G. Circuit switching under the radar with reactor. In *NSDI* (2014).
- [25] LIU, Y. J., GAO, P. X., WONG, B., AND KESHAV, S. Quartz: a new design element for low-latency dcns. In *SIGCOMM* (2014).
- [26] MCKEOWN, N., ANDERSON, T., BALAKRISHNAN, H., PARULKAR, G., PETERSON, L., REXFORD, J., SHENKER, S., AND TURNER, J. Openflow: enabling innovation in campus networks. *ACM SIGCOMM Computer Communication Review* 38, 2 (2008), 69–74.
- [27] PERRY, J., OUSTERHOUT, A., BALAKRISHNAN, H., SHAH, D., AND FUGAL, H. Fastpass: A centralized zero-queue datacenter network. In *SIGCOMM* (2014).
- [28] PORTER, G., STRONG, R., FARRINGTON, N., FORENCICH, A., CHEN-SUN, P., ROSING, T., FAINMAN, Y., PAPAN, G., AND VAHDAT, A. Integrating microsecond circuit switching into the data center. In *SIGCOMM* (2013).
- [29] SHIN, J.-Y., SIRER, E. G., WEATHERSPOON, H., AND KIROVSKI, D. On the feasibility of completely wireless datacenters. *IEEE/ACM Transactions on Networking (TON)* 21, 5 (2013), 1666–1679.
- [30] SHIN, J.-Y., WONG, B., AND SIRER, E. G. Small-world datacenters. In *Proceedings of the 2nd ACM Symposium on Cloud Computing* (2011), ACM, p. 2.
- [31] SINGLA, A., GODFREY, P. B., AND KOLLA, A. High throughput data center topology design. In *NSDI* (2014).
- [32] SINGLA, A., HONG, C.-Y., POPA, L., AND GODFREY, P. B. Jellyfish: Networking data centers randomly. In *NSDI* (2012).
- [33] WANG, G., ANDERSEN, D. G., KAMINSKY, M., PAPAGIANNAKI, K., NG, T., KOZUCH, M., AND RYAN, M. c-through: Part-time optics in data centers. In *SIGCOMM* (2010).
- [34] WANG, W., WANG, Y., LI, X.-Y., SONG, W.-Z., AND FRIEDER, O. Efficient interference-aware tdma link scheduling for static wireless networks. In *MOBICOM* (2006).
- [35] WANG, Y., WANG, W., LI, X.-Y., AND SONG, W.-Z. Interference-aware joint routing and tdma link scheduling for static wireless networks. *IEEE Transactions on Parallel and Distributed Systems (TPDS)* 19, 12 (2008), 1709–1726.
- [36] XU, X., LI, X.-Y., WAN, P.-J., AND TANG, S. Efficient scheduling for periodic aggregation queries in multihop sensor networks. *IEEE/ACM Transactions on Networking (TON)* 20, 3 (2012), 690–698.
- [37] YU, M., GREENBERG, A. G., MALTZ, D. A., REXFORD, J., YUAN, L., KANDULA, S., AND KIM, C. Profiling network performance for multi-tier data center applications. In *NSDI* (2011).
- [38] ZHOU, X., ZHANG, Z., ZHU, Y., LI, Y., KUMAR, S., VAHDAT, A., ZHAO, B. Y., AND ZHENG, H. Mirror mirror on the ceiling: flexible wireless links for data centers. In *SIGCOMM* (2012).
- [39] ZHU, Y., ZHOU, X., ZHANG, Z., ZHOU, L., VAHDAT, A., ZHAO, B. Y., AND ZHENG, H. Cutting the cord: a robust wireless facilities network for data centers. In *MOBICOM* (2014).